Journal of Experimental Nanoscience
Publication details, including instructions for authors and subscription information:
http://www.informaworld.com/smpp/title~content=t716100757

Hydrothermal synthesis and luminescent properties of $GdVO_4$: Eu^{3+} nanophosphors

Bing Yan[a]; Jian-Feng Gu[a]
[a] Department of Chemistry, Tongji University, Shanghai 200092, China

To cite this Article Yan, Bing and Gu, Jian-Feng(2009) 'Hydrothermal synthesis and luminescent properties of $GdVO_4$: Eu^{3+} nanophosphors', Journal of Experimental Nanoscience, 4: 4, 301 — 311
To link to this Article: DOI: 10.1080/17458080903115346
URL: http://dx.doi.org/10.1080/17458080903115346

Journal of Experimental Nanoscience
Vol. 4, No. 4, December 2009, 301–311

Taylor & Francis
Taylor & Francis Group

Hydrothermal synthesis and luminescent properties of $GdVO_4:Eu^{3+}$ nanophosphors

Bing Yan* and Jian-Feng Gu

Department of Chemistry, Tongji University, Siping Road 1239, Shanghai 200092, China

(*Received 15 December 2008; final version received 13 June 2009*)

Eu^{3+}-doped $GdVO_4$ has been synthesised via hydrothermal method by altering the hydrothermal temperature, reaction time and surfactant. The microstructure and morphology information of the phosphors were investigated via the techniques of X-ray powder diffraction and scanning electronic microscopy, which show that the phosphors wear tetragonal phase and the products present various regular morphologies under different reaction conditions such as bulk and nanoparticle. Moreover, the morphologies of the products have been controlled by altering reaction temperature. In addition, the surfactant was also included to control the morphologies of the products and the phosphors present different morphologies. All the phosphors exhibit the characteristic fluorescence of Eu ion ($^5D_0 \rightarrow {}^7F_2$ and $^5D_0 \rightarrow {}^7F_2$). The electric dipole transition $^5D_0 \rightarrow {}^7F_2$ of Eu^{3+} is dominant indicating that most sites of Eu^{3+} ions in $GdVO_4$ have no inversion centre. Furthermore, we found that the reaction time and the morphologies have great influence on optical properties.

Keywords: hydrothermal synthesis; gadolinium vanadate; europium ion; photoluminescence

1. Introduction

Rare earth luminescent materials have considerable practical applications in almost any devices involving the artificial production of light, such as cathode ray tubes, lamps and X-ray detectors [1–7]. Europium ion is widely used as luminescent centre in much phosphors for the exhibited characteristic red emission corresponding to its $^5D_0 \rightarrow {}^7F_2$ transition [8,9]. For example, during the past, the Eu^{3+}-activated YVO_4 attracted attentions because of its broad application [10]. However, due to certain imperfect performance in luminescent intensity and colour purity of the current commercial phosphors much continuous work on the development of new high efficient phosphors still needs to be carried out. Recently, YVO_4 based phosphors have been synthesised by solid-state reaction methods [11–14], spray pyrolysis technique [15] and *in situ* co-precipitation process [16]. In addition to this, some researchers have prepared the nanoparticle of vanadate using co-precipitation and hydrothermal methods [17,18].

*Corresponding author. Email: byan@tongji.edu.cn

ISSN 1745–8080 print/ISSN 1745–8099 online

DOI: 10.1080/17458080903115346
http://www.informaworld.com

As for the hosts, gadolinium vanadate ($GdVO_4$) is also a promising material for rare earth-activated oxide phosphors and near-infrared lasers. $GdVO_4:Eu^{3+}$ used as laser material has been extensively studied [19,20]. In the field of luminescent material, phosphors based on gadolinium compounds also play an important role because the Gd^{3+} ion has its lowest excited levels at relatively high energy, which is due to the stability of the half-filled shell ground state [21,22]. Traditional synthesis methods for rare earth vanadate luminescent materials were solid-state reactions at temperatures above 1300 K or simple wet-chemical technologies, such as chemical co-precipitation, sol–gel and colloidal reactions [23,24].

It is well known that the macroscopic properties of functional material systems with optical, magnetic and electronic properties are highly dependent on the sizes, morphologies, crystal types and compositions [25–28]. The materials may furthermore be of great application for their novel properties induced by reduced dimensionalities. Therefore, there are many reports on the synthesis of nano and microscaled phosphors of one-dimensional (1D) structures, such as wires or rods, tubes, coaxial cables and belts or ribbons, and of complex architectures based on 1D structure, such as branches, urchins and networks [29–32]. Thermal evaporation, laser ablation, metalorganic chemical vapour deposition (MOCVD) and molecular beam epitaxy (MBE) have been used to control the size and morphologies of materials [33–35]. The best solution to control the crystal size and morphology is to employ soft chemistry routes and in particular the hydrothermal processes, which are employed widely in the synthesis of rare earth ions – doped inorganic compounds. For instance, yttrium vanadate, lanthanum fluoride, lanthanum phosphate and yttrium oxide nanoparticles have been successfully prepared via this method [36–38].

In this article, we describe the synthesis and the luminescent properties of $GdVO_4:Eu^{3+}$ via the facile, mild, reproducible and easily controlled hydrothermal route. It is well known that the reaction temperature and time have great influence on the sizes and morphologies of the products. Herein, we have obtained different morphologies of luminescent materials by altering reaction temperature and time or adding surfactant. Moreover, it was found that all the factors influenced the final morphologies of the products. At the same time, we have compared the luminescent properties of these phosphors prepared under different conditions, indicating that the luminescent intensities are dependent on sizes and morphologies of the products.

2. Experimental section

2.1. *Preparation of $GdVO_4:Eu^{3+}$*

The initiative materials were Gd_2O_3, Eu_2O_3 and NH_4VO_3. First, Eu_2O_3 and Gd_2O_3 were added into concentrated nitric acid and heated until they were ropy to obtain $Gd(NO_3)_3$ and $Eu(NO_3)_3$. Then $GdVO_4:Eu^{3+}$ phosphors were synthesised under different conditions via the hydrothermal process, which is described as follows: $Gd(NO_3)_3 \cdot 6H_2O$ (2.0 mmol/0.902 g) and $Eu(NO_3)_3 \cdot 6H_2O$ (0.10 mmol/0.045 g) obtained above were mixed with appropriate amount of NH_4VO_3 (2.0 mmol/0.234 g) in distilled water to form the suspension liquid, and then the pH value was adjusted to 12. Subsequently, the solution was transferred into a Teflon lined stainless steel autoclave. Then the autoclave was sealed and maintained at 170°C for 3 days and 2 days, respectively and then cooled to room temperature in air. The resulting $GdVO_4:Eu^{3+}$ products were filtered, washed with

distilled water and absolute alcohol thrice to remove ions possibly remaining in the final products, and finally dried at 80°C in air for further characterisation.

At the same time, the same process was employed in the synthesis of $GdVO_4:Eu^{3+}$ products at 100°C for 3 days. Besides, by adding the surfactant the products wearing different morphologies have been prepared. The process is described as follows: $Gd(NO_3)_3 \cdot 6H_2O$ (2.0 mmol/0.902 g) and $Eu(NO_3)_3 \cdot 6H_2O$ (0.10 mmol/0.045 g) were mixed with appropriate amount of NH_4VO_3 (2.0 mmol/0.234 g) in distilled water, and then the surfactant was added, stirred for about an half hour to form the suspension liquid and other steps were similar to the above process.

2.2. *Characterisation*

The X-ray powder diffraction (XRD) patterns of all samples were performed on a Bruke/D8-Advance with CuK radiation ($\lambda = 1.518$ Å). The operating voltage and current were maintained at 40 kV and 40 mA, respectively. The scanning electronic microscopic images were obtained with Philips XL-30. The excitation and emission spectra were recorded with a Perkin-Elmer LS-55 model fluorometer equipped with a 150 W xenon lamp as the excitation source. Fourier transform infrared (FTIR) spectroscopy analysis was carried out using KBr discs in the region 4000–400 cm^{-1} by using FTIR–Bruker–EQUINOX–55 under ambient condition. Ultraviolet-visible absorption spectra of the powder were recorded with a lambda 40 spectrometer (Perkin-Elmer). All the measurements were performed at room temperature.

3. Results and discussion

Figure 1 presents the selected XRD patterns of $GdVO_4:Eu^{3+}$ phosphor via the hydrothermal synthesis with (A) or without (B) CTAB surfactant. The X-ray-diffraction peaks of both the products are consistent with the literature data in the JCPDS file (No.17-0260), indicating that we obtained the $GdVO_4:Eu^{3+}$ powders with tetragonal phase, belonging to space group 141/*amd*(141) (lattice constants: $a = 7.213$ Å, $b = 7.213$ Å, $c = 6.367$ Å). The calculated size of the nanoparticles is 45–80 nm using Scherrer's equation, which delegates the dimension and is consistent with the scanning electron microscopy (SEM) observation. By comparing the sample A with CTAB and the sample B without CTAB, no apparent distinction could be found. The crystal phase did not change much under different reaction conditions, and all the curves exhibited very similar characters, so we just gave XRD patterns selectively. The same microstructure may lead to similar morphology.

We also examined the selected FTIR spectra of the $GdVO_4:Eu^{3+}$ phosphor (Figure 2). The bands at 3450 cm^{-1} and 1635 cm^{-1} are assigned to O–H stretching vibration and H–O–H bending vibration, respectively [39]. The two bands are the characteristic vibrations of water from air, physically absorbed on the sample surface, which is completely different from coordinated water in compounds. The V–O stretching vibration bands are designed at the 950–880 cm^{-1} region and the O–V–O asymmetric vibration band at about 560 cm^{-1}.

The morphologies of the samples were obtained by SEM. Figure 3 shows the SEM images of $GdVO_4:Eu^{3+}$ phosphors ((a) and (b) under heating at 170°C for 2 and 3 days, respectively). It can be seen that all the products mainly consist of solid microcrystalline

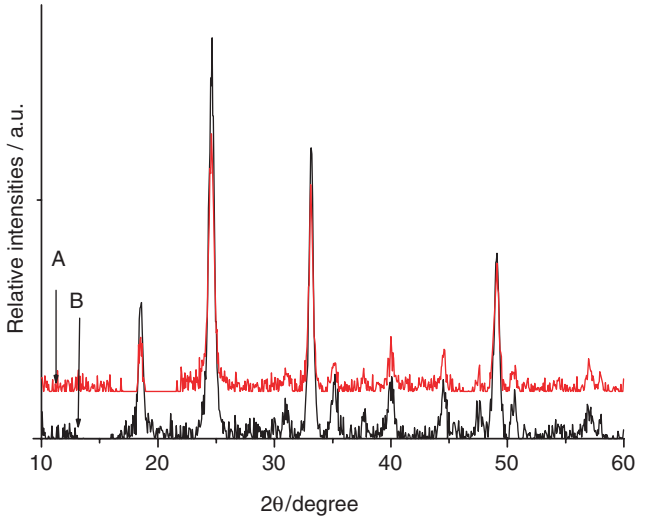

Figure 1. Selected XRD pattern of $GdVO_4:Eu^{3+}$ phosphor at 170°C for 3 days: (A) with 0.06 g CTAB and (B) without CTAB.

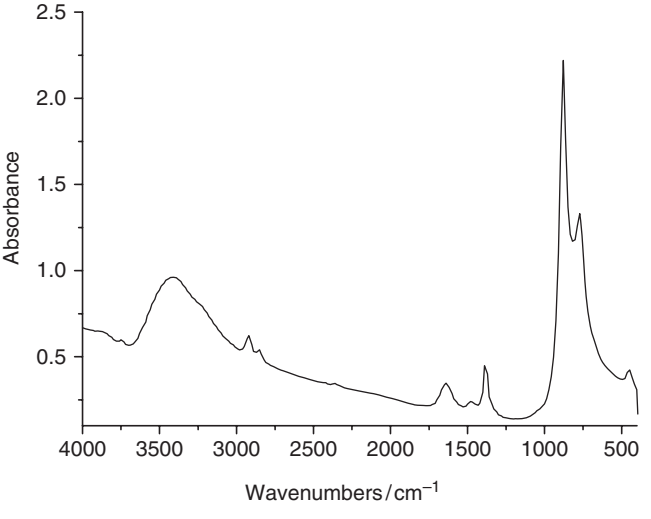

Figure 2. Selected IR spectrum of $GdVO_4:Eu^{3+}$ phosphor at 170°C for 3 days with 0.1 g CTAB.

structures, which show some conglomeration phenomena. While the reaction temperature was 170°C, the grain size is not homogeneously dispersed. At the same time, we also synthesised $GdVO_4:Eu^{3+}$ phosphors under 100°C, the SEM of which is shown in Figure 3(c). From Figure 3(b) and (c), it can be seen that the products present bulk morphology conglomerating with nanoflake and the particle size did not change much with altering temperature. It is well known that any change in the hydrothermal conditions, such as solvents, time, pH value, reaction temperature, will change the size and

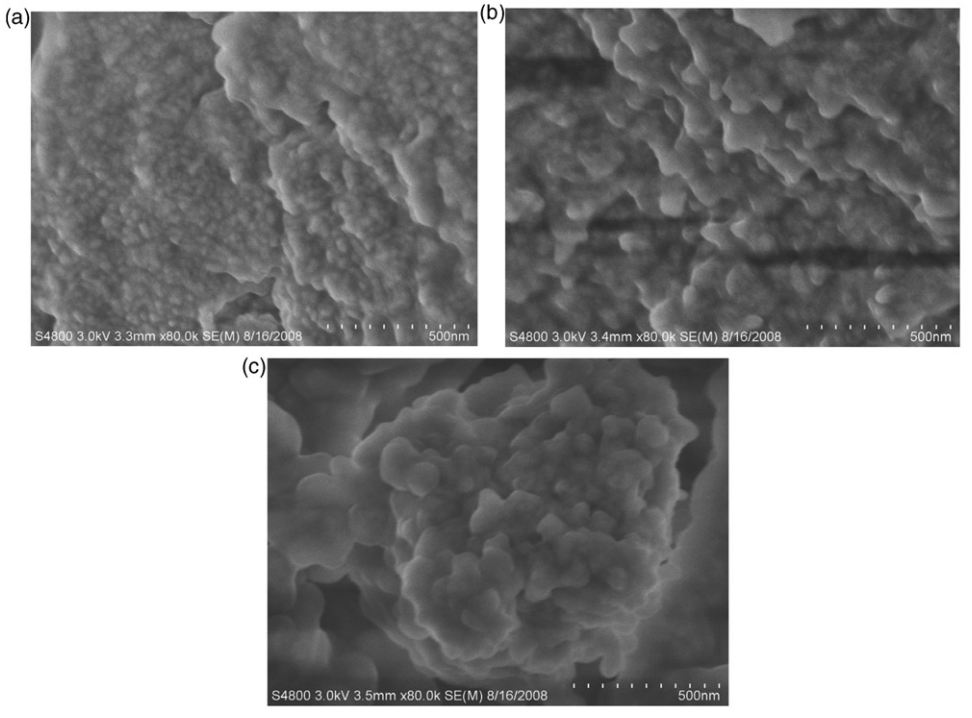

Figure 3. Selected SEM images of $GdVO_4:Eu^{3+}$ phosphors: (a) 170°C, 2 days; (b) 170°C, 3 days and (c) 100°C, 3 days.

morphology of the product. From the above discussion, we can conclude that the influence of both reaction temperature and reacting time is not obvious. The picture shows some nanoparticles with particle size 50–100 nm, which is in agreement with the estimation from XRD.

During the hydrothermal process, the control in the particle size and morphologies not only depend on the inherent structural characteristics of the compounds but also on external experimental conditions, including reaction time, reaction temperature, surfactants and solvents. Therefore, the surfactant is also a key factor for controlling the morphologies of the products (Figure 4(a), (b) and (c)). The product presents the different morphologies heated at 170°C for 3 days in the presence of CTAB. In the hydrothermal process, the surfactants can be used as templates; they may form the spherical micelles and then play the role of the template leading to the products with the nanoparticle morphologies. As a result, the product obtained in the presence of the surfactant shows nanograin morphologies. The morphology of a crystal is the result of the relative growth rates of its different faces, the general rule being that the faces, which grow very slowly, are expressed in the crystal habit. The growth rates of the various crystal faces are determined by intermolecular interactions between molecules in the crystal as well as by a number of external parameters such as solvent, degree of supersaturating, duration, temperature and foreign materials. Any one of these may lead to dramatic modifications in crystal morphology [40].

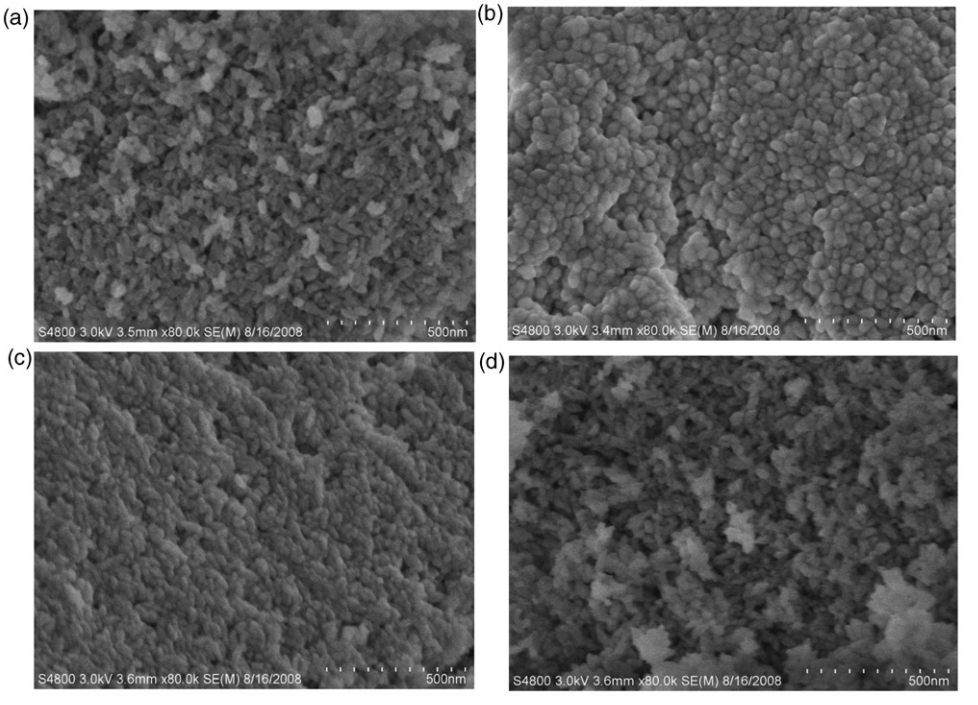

Figure 4. Selected SEM images of $GdVO_4:Eu^{3+}$ phosphors: (a) 170°C, 0.2 g CTAB, 3 days; (b) 170°C, 0.06 g CTAB, 3 days; (c) 170°C, 0.1 g CTAB, 2 days and (d) 100°C, 0.1 g CTAB, 2 days.

The absorption spectra of $GdVO_4:Eu^{3+}$ phosphors have been examined (Figure 5(a)), and involve several bands. The strong band peaking at 280 nm was ascribed to the absorption band of charge transfer band (CTB) (O–Eu) and a weaker band originating from the Eu^{3+} f–f transitions was also observed in the region 300–400 nm, which agreed with the excitation spectra. Besides, in the visible-light region negative absorption of 610 nm is due to the $^5D_0 \rightarrow {}^7F_2$ transition of Eu^{3+} ion. The different morphologies of the phosphors may have influence on the optical properties. The excitation mission and emission spectra of $GdVO_4:Eu^{3+}$ phosphors are shown in Figure 5(b). All the excitation spectra of $GdVO_4:Eu^{3+}$ phosphors were taken at an emission wavelength of 613 nm. All the curves exhibited very similar characters, so we just gave one excitation spectrum selectively (Figure 5(b)). A broad band was observed in the shorter wavelength region from 220 to 280 nm in the excitation spectrum, originating from a charge transfer (CT) transition, as shown in Figure 5(b). This broad band took place by electron delocalisation from an oxygen 2p orbital to an empty 4f orbital of europium ion. It was reported that the peak position of CTB was highly dependent on the Eu–O bond length [41,42]. Besides, the sharp lines in the longer wavelength of 300–400 nm were observed in the spectrum, corresponding to direct excitation of the Eu^{3+} ground state to higher levels of the 4f-manifold, and their assignments are marked in the figure according to the previous work [43].

The emission spectra of all Eu^{3+} activated phosphors have been involved in the following emission lines: $^5D_0 \rightarrow {}^7F_1$, $^5D_0 \rightarrow {}^7F_2$, $^5D_0 \rightarrow {}^7F_3$ and $^5D_0 \rightarrow {}^7F_4$, which are

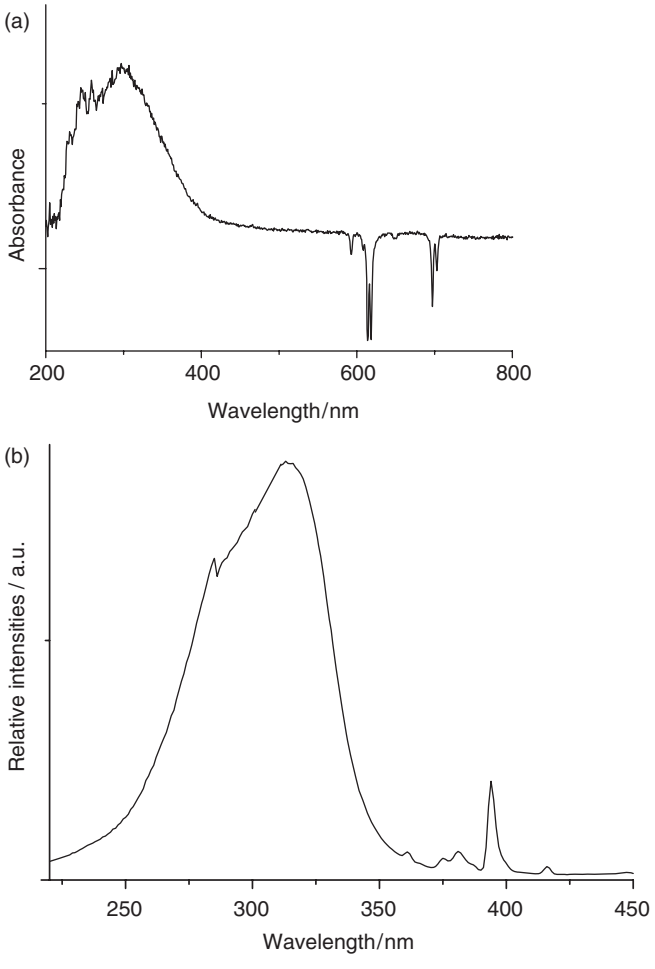

Figure 5. Selected diffuse reflectance ultraviolet visible spectrum (a) and excitation spectrum (b) of $GdVO_4:Eu^{3+}$ phosphor at 170°C for 3 days with 0.1 g CTAB.

determined by transitions between their f-electron energy levels (Figure 6). The orange–red emission lines at around 590 nm originate from the magnetic dipole transition $^5D_0 \rightarrow {}^7F_1$, while the $^5D_0 \rightarrow {}^7F_2$ lines originate from the electric dipole transition. From the emission spectra of $GdVO_4:Eu^{3+}$ phosphors, we can find that peak position of the emission lines are almost the same, but the intensity patterns of their luminescence spectra show some small differences. According to the Judd–Ofelt theory, the magnetic dipole transition is permitted. However, the electric dipole transition is allowed only when the europium ion occupies a site without an inversion centre and the intensity is significantly affected by the symmetry in local environments around Eu^{3+} ions [44]. If the Eu^{3+} ions occupy an inversion symmetry site in the $GdVO_4$ crystal lattice, the orange–red emission, magnetic transition $^5D_0 \rightarrow {}^7F_1$ (around 590 nm), is the dominant transition. In contrast, the electric

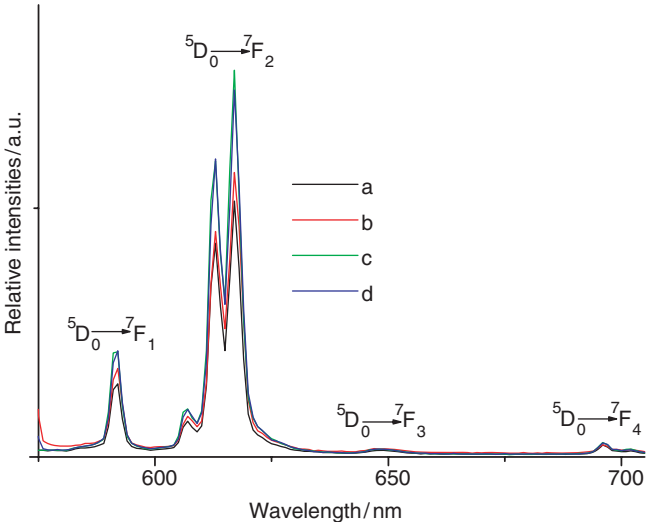

Figure 6. Emission spectra of $GdVO_4$: Eu^{3+} phosphors at 170°C for 3 days with different CTAB: (a) 0.2 g CTAB; (b) 0.4 g CTAB (c) 0.6 g CTAB and (d) 0.1 g CTAB.

dipole transition $^5D_0 \rightarrow {}^7F_2$ (around 610–620 nm) is the dominant transition. According to the emission spectra, it can be concluded that most Eu^{3+} ions have no inversion centres and the electric dipole transition $^5D_0 \rightarrow {}^7F_2$ is dominant. Due to the interaction between Eu^{3+} and O^{2-} ions in $GdVO_4$ doped with Eu^{3+}, level split can be caused by the crystal field and a little split of Eu^{3+} emission bands has been observed. From Figure 7(a), it can be seen that the optical property is enhanced when the amount of the surfactant increases. We surmised that the result is relative to the morphologies and sizes of the products. The three-dimensional sizes of crystalline grain are very thick to afford high strength. It needs to be referred that the crystalline powder and micrometre dimension for these powders with high strength would be very useful for the application to obtain high efficient phosphors because these microcrystalline materials can result in high luminescent intensities [45]. We also investigated the influence of the reaction time on the optical property (Figure 7(b)) and found that the reaction time has no obvious influence on the optical property. This can be ascribed to the similar morphologies of the phosphors.

4. Conclusions

In summary, Eu^{3+}-doped gadolinium vanadium oxides ($GdVO_4:Eu^{3+}$) with tetragonal phase have been synthesised via hydrothermal method. The products present various regular morphologies under different reaction conditions such as bulk, nanorod and nanoparticle. Moreover, the morphologies of the products have been controlled successfully by altering reaction temperature. The surfactant was also included to control the morphologies of the products and the presence of surfactant can avoid conglomeration phenomena. All the phosphors exhibit the characteristic fluorescence of Eu ion. The electric dipole transition $^5D_0 \rightarrow {}^7F_2$ of Eu^{3+} ions is dominant indicating that most sites of

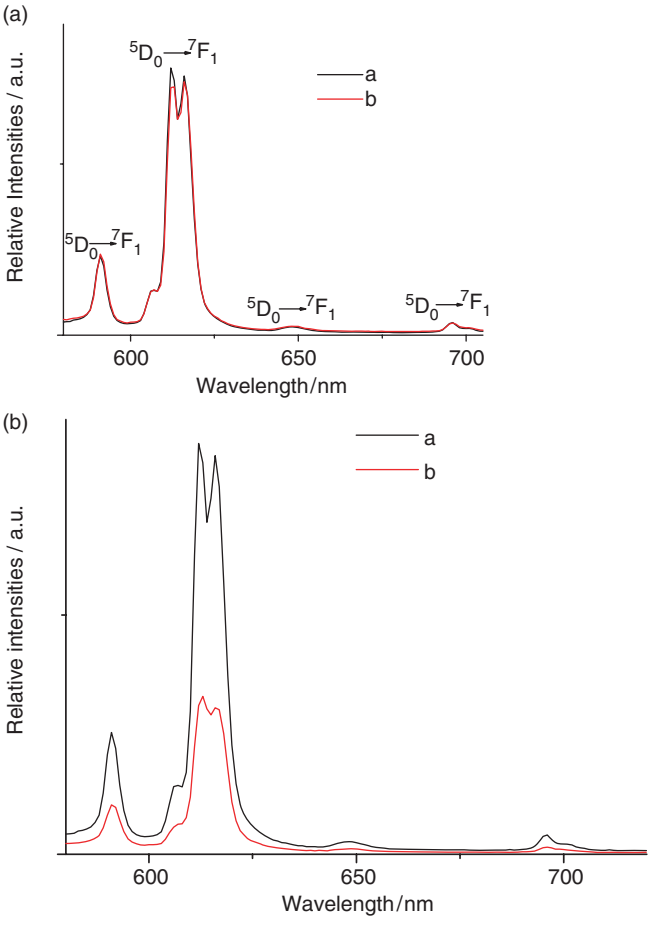

Figure 7. Selected emission spectra of $GdVO_4:Eu^{3+}$ phosphors: (a) 170°C for different time. (a) 2 days; (b) 3 days and (b) at different temperature for 3 days (a) 170°C; (b) 100°C.

Eu^{3+} ions in $GdVO_4$ have no inversion centre. Furthermore, we found that the relatively small particle size and regular morphology are favourable for the optical properties.

References

[1] G. Blasse and B.C. Grabmeter, *Luminescent Materials*, Springer-Verlag, Berlin, Germany, 1994.
[2] K. Riwotzki and M. Haase, *Colloidal YVO_4: Eu and $YP_{0.95}V_{0.05}O_4$: Eu nanoparticles: Luminescence and energy transfer processes*, J. Phys. Chem. B 105 (2001), pp. 12709–12713.
[3] O. Chukova, S. Nedilko, Z. Moroz, and M. Pashkovskyi, *Luminescence of the samarium ions doped in the complex oxides with heterovalence substitution*, J. Lumin. 102–103 (2003), pp. 498–503.
[4] H.F. Brito, O.L. Malta, and M.C.F.C. Felinto, *Luminescent properties of diketonates of trivalent europium with dimethyl sulfoxide*, J. Alloys Compounds 344 (2002), pp. 293–297.

[5] R. Reisfeld, M. Zelner, and A. Patra, *Fluorescence study of zirconia films doped by Eu^{3+}, Tb^{3+} and $Sm^{3+}$and their comparison with silica films*, J. Alloys Compounds 300–301 (2000), pp. 147–151.
[6] H.J. Zhang, J.Y. Wang, C.Q. Wang, L. Zhu, X.B. Hu, X.L. Meng, M.H. Jiang, and Y.T. Chow, *A comparative study of crystal growth and laser properties of Nd: YVO_4, Nd: $GdVO_4$ and Nd: $Gd_xLa_{1-x}VO_4$ (x−0.80, 0.60 0.45) crystals*, Opt. Mater. 23 (2003), pp. 449–454.
[7] R.X. Yan, X.M. Sun, X. Wang, Q. Peng, and Y.D. Li, *Crystal structuresanisotropic growth, and optical properties*: *Controlled synthesis of lanthanide orthophosphate one-dimensional nanomaterials*, Chem. Eur. J. 11 (2005), pp. 2183–2195.
[8] L.S. Wang, J. Lin, and Z.W. Quan, *Synthesis and characterization of $Y_{0.9-x}Gd_xEu_{0.1}BO_3$ phosphors by spray drying process*, J. Rare Earths 22 (2004), pp. 91–94.
[9] Y.H. Wang, T. Endo, L. He, and C.F. Wu, *Synthesis and photoluminescence of Eu^{3+}-doped (Y,Gd)BO_3 phosphors by a mild hydrothermal process*, J. Cryst. Growth 268 (2004), pp. 568–574.
[10] F.M. Nirwan, T.K. GunduRao, P.K. Gupta, and R.B. Pode, *Studies of defects in YVO_4: Pb^{2+}, Eu^{3+} red phosphor material*, Phys. Status Solidi a 198 (2003), pp. 447–456.
[11] X.Q. Su and B. Yan, *Matrix-induced synthesis and photoluminescence of $M_3Ln(VO_4)_3$: RE (M = Ca, Sr, Ba; Ln = Y, Gd; RE = Eu^{3+}, Dy^{3+}, Er^{3+}) phosphors by hybrid precursors*, J. Alloys Compounds 421 (2006), pp. 273–278.
[12] S.J. Yang, L.J. Yuan, and J.T. Sun, *Synthesis and luminescent properties of Eu^{3+}-doped $Na_{24}AS_2W_{22}O_{83}$*, Rare Metals 22 (2003), pp. 95–97.
[13] C.P. Frank, K.L. Albert, and R. Maija, *Rare Earth Activated phosphors based on yttrium orthovanadate and related compounds*, J. Electrochem. Soc. 112 (1965), pp. 776–779.
[14] U. Rambabu, D.P. Amalnerkar, B.B. Kale, and S. Buddhudu, *Fluorescence spectra of Eu^{3+}-doped $LnVO_4$ (Ln = La and Y) powder phosphors*, Mater. Res. Bull. 35 (2000), pp. 929–936.
[15] Y.H. Zhou and J. Lin, *Luminescent properties of YVO_4: Dy^{3+} phosphors prepared by spray pyrolysis*, J. Alloys Compounds 408 (2006), pp. 856–859.
[16] B. Yan and X.Q. Su, *The synthesis and luminescence of $YP_xV_{1-x}O_4$: Dy^{3+} microcrystalline phosphors by in situ co-precipitation composition of hybrid precursors*, Mater. Chem. Phys. 93 (2005), pp. 552–556.
[17] K. Riwotzki and M. Haase, *Wet-chemical synthesis of doped colloidal nanoparticles: YVO_4: Ln (Ln = Eu, Sm, Dy)*, J. Phys. Chem. B 102 (1998), pp. 10129–10135.
[18] A. Huignard, T. Gacoin, and J.P. Boilot, *Synthesis and luminescence properties of colloidal YVO_4: Eu phosphors*, Chem. Mater. 12 (2000), pp. 1090–1094.
[19] H.D. Jiang, H.J. Zhang, J.Y. Wang, H.R. Xia, X.B. Hu, B. Teng, and C.Q. Zhang, *Optical and laser properties of Nd: $GdVO_4$ crystal*, Opt. Commun. 198 (2000), pp. 447–452.
[20] S. Osawa, T. Katsumata, T. Iyoda, Y. Enoki, S. Komuro, and T. Morikawa, *Effects of composition on the optical properties of doped and nondoped $GdVO_4$*, J. Cryst. Growth 198/199 (1999), pp. 444–448.
[21] X.Q. Su, B. Yan, and H.H. Huang, *In situ co-precipitation synthesis and luminescence of $GdVO_4$: Eu^{3+} and $YxGd_{1-x}VO_4$: Eu^{3+} microcrystalline phosphors derived from the assembly of hybrid precursors*, J. Alloys Compounds 399 (2005), pp. 251–255.
[22] A.M. Pires, M.R. Davolos, and E.B. Stucchi, *Thermal decomposition and rehydration of strontium oxalate: Morphological evolution*, Int. J. Inorg. Mater. 3 (2001), pp. 785–790.
[23] Y.Q. Yu, S.H. Zhou, and S.Y. Zhang, *Luminescence of the compounds $Y_{0.5-x}$ $Li_{1.5}VO_4$: ($Dy^{3+}Eu^{3+}$)*, J. Alloys Compounds 351 (2003), pp. 84–86.
[24] E. Cavalli, M. Bettinelli, A. Belletti, and A. Speghin, *Optical spectra of yttrium phosphate and yttrium vanadate single crystals activated with Dy^{3+}*, J. Alloys Compounds 341 (2002), pp. 107–110.
[25] J. Joo, T. Yu, Y.W. Kim, H.M. Park, F. Wu, J.Z. Zhang, and T. Hyeon, *Multigram scale synthesis and characterization of monodisperse tetragonal zirconia nanocrystals*, J. Am. Chem. Soc. 125 (2003), pp. 6553–6557.

[26] D. Boyer and R. Mahiou, *Powders and coatings of $LiYF_4$: Eu^{3+} obtained via an original way based on the sol-gel process*, Chem. Mater. 16 (2004), pp. 2518–2521.
[27] L.X. Yu, H.W. Song, S.Z. Lu, Z.X. Liu, L.M. Yang, and X.K. Kong, *Luminescent properties of LaPO4: Eu nanoparticles and nanowires*, J. Phys. Chem. B 108 (2004), pp. 16697–16702.
[28] C.J. Jia, L.D. Sun, L.P. You, X.C. Jiang, F. Luo, Y.C. Pang, and C.H. Yan, *Selective synthesis of monazite- and zircon-type $LaVO_4$, nanocrystals*, J. Phys. Chem. B 109 (2005), pp. 3284–3290.
[29] L. Vayssieres, *Growth of arrayed nanorods and nanowires of ZnO from aqueous solutions*, Adv. Mater. 15 (2003), pp. 464–466.
[30] B. Yan, X.Q. Su, and K. Zhou, *In situ chemical coprecipatation composition of hybrid precursors to red YVO4: Eu^{3+} and green $LaPO_4$: Tb^{3+} phosphors*, Mater. Res. Bull. 41 (2006), pp. 134–143.
[31] G. Shen G, Y. Bando, and C.J. Lee, *Synthesis and evolution of novel hollow ZnO urchins by a simple thermal evaporation process*, J. Phys. Chem. B 109 (2005), pp. 10578–10583.
[32] C.X. Xu, X.W. Sun, B.J. Chen, Z.L. Dong, M.B. Yu, X.H. Zhang, and S.J. Chua, *Network array of zinc oxide whiskers*, Nanotechnology 16 (2005), pp. 70–73.
[33] J.Q. Hu, Q. Li, X.M. Meng, C.S. Lee, and S.T. Lee, *Thermal reduction route to the fabrication of coaxial Zn/ZrO nanocables and ZnO nanotubes*, Chem. Mater. 15 (2003), pp. 305–308.
[34] B. Yan and X.Q. Su, *In situ co-precipitation synthesis and photoluminescence of $Y_xGd_{1-x}VO_4$: Tm^{3+} microcrystalline phosphors by hybrid precursors*, Opt. Mater. 29 (2007), pp. 1866–1870.
[35] X.H. Zhang, Y.C. Liu, X.H. Wang, S.J. Chen, G.R. Wang, J.Y. Zhang, Y.M. Lu, D.Z. Shen, and X.W. Fan, *Structural properties and photoluminescence of ZnO nanowalls prepared by two-step growth with oxygen-plasma-assisted molecular beam epitaxy*, J. Phys.: Condens. Matter 17 (2005), pp. 3035–3042.
[36] A. Huignard, V. Buissette, G. Laurent, T. Gacoin, and J.P. Boilot, *Synthesis and characterizations of YVO_4: Eu colloids*, Chem. Mater. 14 (2002), pp. 2264–2269.
[37] A. Huignard, V. Buissette, A.C. Franville, T. Gacoin, and J.P. Boilot, *Emission processes in YVO_4:Eu nanoparticles*, J. Phys. Chem. B 107 (2003), pp. 6754–6759.
[38] J.W. Stouwdam and F.C.J.M Van Veggel, *Near-infrared emission of redispersible Er^{3+} Nd^{3+}, and Ho^{3+} doped LaF_3 nanoparticles*, Nano Lett. 2 (2002), pp. 733–737.
[39] A. Kato, S. Oishi, T. Shishido, M. Yamazaki, and S. Iida, *Evaluation of stoichiometric rare-earth molybdate and tungstate compounds as laser materials*, J. Phys. Chem. Solids 66 (2005), pp. 2079–2081.
[40] K. Byrappa, C.K. Chandrashekar, B. Basavalingu, K.M. Lokanatharai, S. Ananda, and M. Yoshimura, *Growth, morphology and mechanism of rare earth vanadate crystals under mild hydrothermal conditions*, J. Cryst. Growth 306 (2007), pp. 94–101.
[41] Z.G. Wei, L.D. Sun, C.S. Liao, J. Yin, X. Jiang, and C.H. Yan, *Size-dependent chromaticity in YBO_3: Eu nanocrystals: Correlation with microstructure and site symmetry*, J. Phys. Chem. B 106 (2002), pp. 10610–10617.
[42] C.F. Wu, W.P. Qin, G.S. Qin, D. Zhao, J.S. Zhang, S.H. Huang, S.Z. Lu, H.Q. Liu, and H.Y. Lin, *Photoluminescence from surfactant-assembled Y_2O_3: Eu nanotubes*, Appl. Phys. Lett. 82 (2003), pp. 520–522.
[43] H. Meyssamy, K. Riwotzki, A. Kornowski, S. Naused, and M. Haase, *Wet-chemical synthesis of doped colloidal nanomaterials: Particles and fibers of $LaPO_4$: Eu $LaPO_4$: Ce, and $LaPO_4$: Ce, Tb*, Adv. Mater. 11 (1999), pp. 840–844.
[44] J. Dexpert-Ghys, R. Mauricot, and M.D. Faucher, *Spectroscopy of Eu^{3+} ions in monazite type lanthanide orthophosphates $LnPO_4$ Ln = La or Eu*, J. Lumin. 27 (1996), pp. 203–215.
[45] B. Yan and X.Q. Su, *$LuVO_4$: RE^{3+} (RE = Sm, Eu, Dy, Er), phosphors by in-situ chemical precipitation construction of hybrid precursors*, Opt. Mater. 29 (2007), pp. 547–551.